ASME Journal of Engineering for Sustainable Buildings and Cities
Online journal at:
https://asmedigitalcollection.asme.org/sustainablebuildings

Effect of Nonthermal Plasma Technology on Reducing Airborne Contaminants in an Indoor Setting

Deify Law[1]
Department of Mechanical Engineering,
California State University, Fresno,
2320 E. San Ramon Ave. M/S EE94,
Fresno, CA 93740-8030
e-mail: dlaw@csufresno.edu

Elbert Ho
Department of Mechanical Engineering,
California State University, Fresno,
2320 E. San Ramon Ave. M/S EE94,
Fresno, CA 93740-8030
e-mail: elbert@mail.fresnostate.edu

A variety of air cleaning technologies have been used to reduce airborne contaminants consisting of particulates and gaseous pollutants in an indoor environment over the past several decades. Air cleaning technologies have the potential of assisting low-cost fibrous media to clean contaminated indoor air and reduce building ventilation rates to conserve energy. Air cleaning technologies including plasma air ionization, photocatalytic oxidation, sorption, ultraviolet, electrostatic precipitator, high-efficiency particulate air (HEPA), activated carbon, etc. are employed to reduce, capture, or eliminate airborne contaminants. The plasma air ionization method generally turns electrically neutral air into negative or bipolarized air ions by applying an electric charge to the indoor air to produce a clean indoor air environment. There are two types of plasma ionization: nonthermal ionization and thermal plasma ionization. Nonthermal plasma ionization includes dielectric barrier discharge (DBD) and needlepoint bipolar ionization (NBI). A growing body of recent evidence has presented the potential of using bipolar air ionization to remove airborne particles and gaseous pollutants, and to decrease bacterial deposition on surfaces, inactivate airborne bacteria, viruses, and fungi. Meanwhile, NBI is where the ions are emitted into the airflow by needles or carbon brushes or other needlepoint-type emitters while DBD bipolar ionization uses a sealed cathode tube to create a plasma discharge which will then emit ions into the airflow. The present work particularly studies the effect of DBD bipolar ionizer-assisted minimum efficiency reporting value (MERV) filter technology on reducing airborne contaminants including particulates and toxic gases.
[DOI: 10.1115/1.4068505]

Keywords: indoor air quality, nonthermal plasma technology, bipolar air ionization, air cleaning technologies

[1]Corresponding author.
Manuscript received December 20, 2024; final manuscript received April 9, 2025; published online July 4, 2025. Assoc. Editor: K. Max Zhang.

1 Introduction

Indoor air quality is an indispensable measure for ensuring a clean indoor environment in sustaining occupant health, comfort, and productivity and is generally measured by the concentrations of particulate matter (PM) and gaseous pollutants. Particulate matter, also known as particulate pollution, is a mixture of solid particles and liquid droplets found in the air [1]. The size of particulate matter ranges from submicrons to microns (μm) in particle diameter. Examples of particulate matter include dust, smoke, dirt, pollens, molds, viruses, fungi, droplets, etc. that suspend in the indoor or outdoor air and generally come from two sources: inhalable particles (PM_{10}) with particle diameters that are 10 μm and smaller and fine inhalable particles ($PM_{2.5}$) with diameters that are 2.5 μm and smaller. Inhalable particles can be detrimental and risky to human health because the matter can get into the lungs and even the bloodstream of a human. Furthermore, gaseous pollutants generally comprise of volatile organic compounds (VOCs), which are organic chemical compounds emitted as gases from certain solids or liquids [2], and non-VOCs such as carbon dioxide emitted by humans. VOCs are highly volatile, mobile, and transportable over long distances [3]. VOCs vaporize easily under normal conditions due to their high vapor pressure or low boiling point in the environment and VOCs can be emitted from outdoor and indoor sources including wildfire, agricultural waste combustion, fossil fuels burning, automobile exhaust, new building materials and furnishings, office equipment, personal hygiene products, paint, etc. Unfortunately, VOCs are highly toxic, and they pose short- and long-term adverse effects to human health when there is a large concentration of or exposure of time to the VOCs by humans.

A variety of air cleaning technologies have been used to reduce airborne contaminants consisting of particulates and gaseous pollutants in an indoor environment over the past several decades. Air treatment technologies have the potential of reducing building ventilation rates to conserve energy. Air cleaning technologies including plasma, photocatalytic oxidation, sorption, ultraviolet, electrostatic precipitator (ESP), high-efficiency particulate air (HEPA), activated carbon, etc. are employed to reduce, capture, or eliminate airborne contaminants [4–8]. There are two types of plasma ionization: nonthermal and thermal plasma ionization. Plasma exists when electrons in molecules are heated to extremely high temperatures and the energized electrons leave the molecule orbits. A nonthermal plasma is basically a plasma that happens at room temperature when the molecules are introduced with a strong electrical field. Nonthermal plasma ionization is primarily used for indoor applications owing to its low ionization intensity and thus, it becomes the focus of the present work. Nonthermal plasma is generated by a strong electric field to create a neutral gas discharge and release electrons, and in turn generate ions and photons, which can generally agglomerate smaller particles and decompose VOCs [9]. Similarly, nonthermal plasma can be generated when electrons are released at high energy with the gaseous atoms and molecules remaining neutral in the atmospheric pressure. The high-energy electrons will then increase the ionization potential of those neutrally charged atoms and molecules to make negative and/or positive ions. Dielectric barrier discharge (DBD) bipolar ionization is a type of nonthermal plasma application. DBD produces highly nonequilibrium, controlled plasmas at atmospheric pressure and can effectively generate atoms, radicals, and energized species with energetic electrons at moderate gas temperatures [10]. The DBD is generally composed of two electrodes, which are separated by insulated material gap spacing. One of the electrodes is covered with a dielectric material [11]. Electron energy released by the DBD ionizer will be used to disassociate the gas molecules and, thereby, to create ions [11].

A growing body of recent evidence has presented the potential of using a nonthermal plasma air cleaning technology, such as unipolar or DBD bipolar air ionization, to remove airborne particles and gaseous pollutants, and to decrease bacterial deposition on surfaces, inactivate airborne bacteria, viruses, and fungi [12–20]. Hobbs et al. [12] reported that a bipolar ionizer suppressed and mitigated particle generation in a clean room environment. Gabbay et al. [13] used a corona discharge ionizing generator to investigate the effect of ions on the microbial air pollution of a dental clinic. Microbial air levels in the dental clinic were significantly reduced with the generator by 40–50%. The data suggested that the ionizing generator can be used to reduce microbial air pollution within the dental clinic, thus reducing the environmental hazard of infections to the staff. Byeon et al. [6] measured the size distributions of bimodal submicron aerosol particles and estimated the collection efficiency of the particles for a hybrid two-stage ESP composed of a DBD charger as the particle charger and an ESP as the charged particle collector. The particle collection efficiencies increased as alternating current applied voltage increased at a fixed frequency and flowrate. Lee et al. [14] evaluated the continuous emission of unipolar ions to determine their ability to remove fine and ultrafine particles from indoor air environments. The study concluded that ionic air purifiers, which can produce unipolar ions, can be efficient in controlling fine and ultrafine aerosol pollutants in indoor air environments. Furthermore, Sherali [15] reported that there was a high concentration rate of aerosol decay with a bipolar ionization unit compared with that of without ionization.

Hyun et al. [16] conducted laboratory tests involving the filtration and inactivation of a bacteriophage MS2 virus using a carbon-fiber ionizer installed upstream of a medium filter. The overall filtration efficiency increased when the ionizer was on and the antiviral efficiency with bipolar ions was higher than that with unipolar ions, but the electric field was not effective for inactivation. Gast et al. [17] applied negative air ionization for reducing experimental airborne transmission of *Salmonella enteritidis* to chicks. Air ionization imparted a negative charge to airborne dust particles and thereby caused them to be attracted to ground surfaces. Reducing airborne dust levels through air ionization offered a powerful tool for restricting the opportunities for Salmonella infections to spread extensively throughout poultry flocks.

Zeng et al. [18] conducted experiments to evaluate the gas and particle removal effectiveness and potential for byproduct formation resulting from the operation of a commercially available in-duct bipolar ionization device. Both the chamber and field tests suggested that the use of the tested bipolar ionization unit led to a decrease in xylenes but an increase in oxygenated VOCs (e.g., acetone and ethanol) and toluene. Kim et al. [19] reviewed and compared various principles and approaches employed in air ionization techniques as a control technology for reducing off-gas emissions of volatile organic compounds. Air ionization techniques were used extensively to remove odors and VOCs from air flows, and the feasibility was demonstrated in sensitive manufacturing operations. The future of air ionization will be brightened by continuing efforts to improve their cost-effectiveness and minimize the production of by-products. Van Durme et al. [20] investigated the effect of catalyst and humidity on both ozone and toluene removal using hybrid plasma catalyst technology. Toluene is a type of VOCs. The tested plasma technology is nonthermal, which is a direct current corona discharge. Ozone removal strongly correlated with the active compound of the tested catalysts whereas the effect of humidity on ozone abatement was negligible for the tested catalysts. Toluene removal efficiency was 90% and 39% at 39% and 74% relative humidity, respectively. Park et al. [11] conducted a lab-scale test of a ventilation system including a DBD ionizer and a UV-photocatalyst filter for simultaneous removal of gaseous and particulate contaminants. The percentage reduction of PM 2.5 was approximately 79.5%. The UV-photocatalyst filter was used to enhance the decomposition of VOC gaseous species, such as formaldehyde (HCHO), benzene, toluene, and xylene (BTX), into carbon dioxide and water vapor products. Both HCHO and BTX were reported to be completely removed in the test [6]. Wu and Lee [21] carried out studies on the removal of VOCs by negative air ions (NAIs). Three species of VOCs—chloroform, toluene, and 1,5-hexadiene—were selected to react with NAI at relative humidities of 0%, 25%, and 70%. The reaction rate constantly declined as the relative humidity increased in the reaction between toluene and NAI, but such a relationship was not evident in the reaction between 1,5-hexadiene and NAI. In addition, Chen et al. [22] degraded formaldehyde by a soft-sliding-electrification-induced air ionization method.

In the present work, the effect of a DBD bipolar ionization device (AtmosAir Solutions FC-400) on the possibility of enhancing a minimum efficiency reporting value (MERV) filter to mitigate airborne contaminants that comprise of particulate matter and gaseous pollutants will be studied and reported. The present work does not study the reduction of microbes. The primary objective of the present work is to investigate if a low-cost MERV filter (e.g., MERV 13) when combined with the DBD bipolar ionizer can approximately reach the particulate removal efficiency of a HEPA filter with the dual purposes of conserving energy due to high pressure drop across a HEPA filter and reducing electrical power cost for sustainability. Furthermore, a HEPA filter is not optimal as a room air filter because of its high particulate removal efficiency, which is associated with higher electrical power cost and noise [23]. The secondary objective is to study the percentage reductions of gaseous pollutants including total volatile organic compounds, formaldehyde, and carbon dioxide gas concentrations due to the DBD bipolar ionization.

2 Materials and Methods

2.1 Experimental Methodology. A stand-alone unoccupied prop house built by the construction program of Fresno City College is used as the test chamber. Figure 1 demonstrates the setup of the present air cleaning test in a prop house. The components of the test setup include both supply and return air flexible/rigid ducts, one indoor air quality sensor, one source injector, one total volatile organic compounds (TVOCs) sensor, one mechanical air filter compartment, one dielectric bipolar ionization technology mounting station, and an air-handling unit. The tightly sealed L-shaped indoor test space enclosed by a thick boundary is shown in Fig. 1. Both Carrier Opticlean and air-handling units are located at the bottom right of the prop house, which is the garage space. The HEPA filter is installed inside the Carrier Opticlean negative air machine unit whereas the combined DBD bipolar ionization and MERV filtration system is placed inside the air-handling unit. There is one small room of the house located approximately toward the bottom center of Fig. 1, which is completely sealed and enclosed, and it is not part of the test study. Additionally, the non-filled and filled arrows indicate the directions of return and supply air in Fig. 1, respectively. The emission source is woodchip-based smoke. The TVOC sensor measures the TVOC concentrations in terms of percentages (%) whereas the indoor air quality sensor records the particle concentrations in count/cm^3, $PM_{2.5}$ and PM_{10} in $\mu g/m^3$, formaldehyde in mg/m^3, and carbon dioxide concentrations in parts per million (ppm). The airflow is maintained with a 100% return air by shutting off the outside air damper of the economizer from the air-handling unit in Fig. 1.

The floor area and the overall volume of the prop house are approximately 37 m^2 and 90 m^3, respectively. The prop house includes a central air conditioning system, and the system uses 100% recirculated air with tightly sealed ductwork. The central air conditioning fan is operated in all experiments. The indoor air cleaning test configuration varies between one of the in-duct MERV filters (e.g., MERV 8 and MERV 13) installed one at a time and with an in-duct DBD bipolar ionization device (AtmosAir

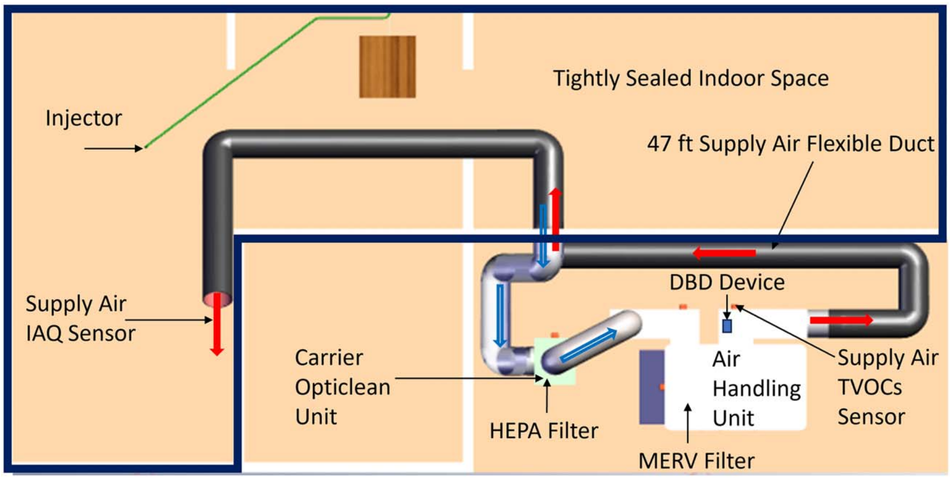

Fig. 1 Setup of the air cleaning test experiment. Non-filled and filled arrows represent return and supply air directions.

Solutions FC-400) either on or off. The in-duct DBD bipolar ionization device uses a sealed cathode tube to create a plasma discharge which will emit ions into the airflow. Indoor air cleaning experiments are carried out to test the effect of DBD bipolar ionization-assisted MERV filter on particulate matter removal efficiency, percent reductions of TVOCs, and decay of formaldehyde and carbon dioxide gas concentrations. The particulate matter removal efficiency will be compared with that of the HEPA filter alone. The prop house is equipped with instruments to monitor indoor particle and gaseous concentrations. The indoor air quality instrumentation system is composed of one TVOC sensor (BELIMO) and one indoor air quality sensor (TSI Q-Trak XP) mounted at the supply air duct location. The indoor air quality sensor measures the particle concentrations, particulate matter (e.g., $PM_{2.5}$ and PM_{10}), carbon dioxide, and formaldehyde concentrations at the supply air location. Each indoor air cleaning configuration test lasts approximately 1 h. All data are logged over a 1-min time resolution during the 1-h test duration. Each test configuration is repeated multiple times, and a general timeline of a test configuration is reported in this section. Source (e.g., woodchip-based smoke) injection system is triggered after 10-min baseline data collection and runs for approximately 5 min. Then, the air conditioning system fan and DBD bipolar ionizer if used are turned on for 30 minutes. Lastly, both the fan and the DBD bipolar ionization device will be turned off and the indoor environment will be left to settle down during the last 15 min of the test duration. All data are then collected and averaged from the repeated measurements at the supply air duct during the last 15-min steady state of each test when both fan and DBD bipolar ionization air cleaning device if used are turned off. The supply air velocity is 6.6 m/s that is measured by a hotwire anemometer (TSI). The supply air duct diameter is 36 cm. The average outdoor air temperature and relative humidity are measured at 90 °F and 20%, respectively. The ion count is measured by an air ion counter (AlphaLab Inc.). While the baseline average ion reading is 0.3×10^3 ions/cm^3 without ionization, the average ion count is 2.5×10^3 ions/cm^3 when the DBD bipolar ionization device is operated. The average ozone level is measured to be 0.003 parts per million (ppm) with ionization operated, which is well below the Environmental Protection Agency (EPA) standard of 0.075 ppm [24]. Additionally, Kang et al. [25] detected nitrogen oxides and peroxides from their nonthermal DBD plasma study. However, those by-products are not detected in the present study.

3 Results and Discussion

3.1 Particulate Matter Study. Figure 2 compares the average $PM_{2.5}$ removal efficiency of the MERV 13 filter assisted with and without DBD bipolar ionization and a stand-alone HEPA filter. The removal efficiency is determined using the following equation:

$$\text{Removal efficiency} = \frac{m_i - m_f}{m_i} \times 100\% \tag{1}$$

where m_i and m_f represent the measured initial and final mass density of $PM_{2.5}$ in μg/m^3 during the air cleaning test period. A full mechanical recirculation system using MERV 13 filter assisted with DBD bipolar ionization technology shows significant improvement in the average $PM_{2.5}$ removal efficiency (97%) when compared with the MERV 13 filter alone without ionization (85%). The $PM_{2.5}$ removal efficiency of the HEPA filter is found to be 99.7% in the present study. According to the strict definition of a HEPA filter, it is at least 99.97% efficient at removing 0.3-μm particles [26], and it has greater efficiency for smaller and larger particles. Results show that the DBD bipolar ionization enhances the $PM_{2.5}$ removal efficiency of the MERV 13 filter to be approximately comparable to that of the HEPA filter alone. Figure 3

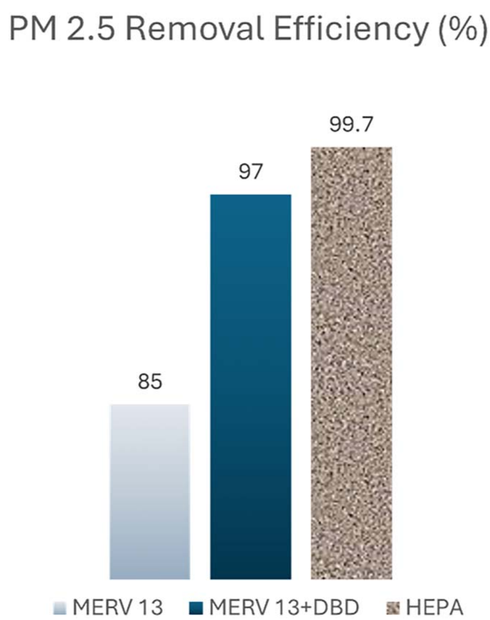

Fig. 2 Comparison of the $PM_{2.5}$ removal efficiency of MERV 13 filter assisted with and without DBD bipolar ionization and a stand-alone HEPA filter

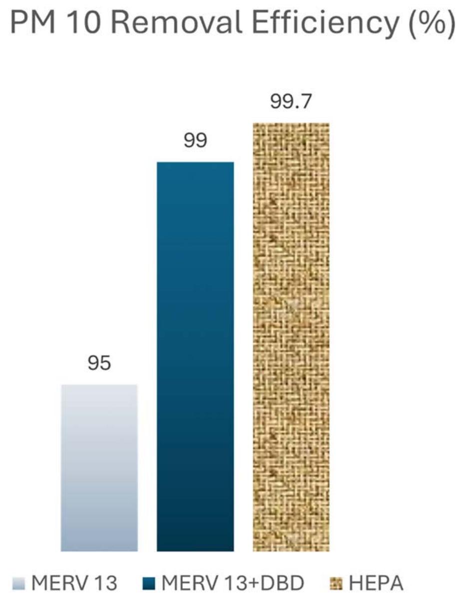

Fig. 3 Comparison of the PM_{10} removal efficiency of MERV 13 filter assisted with and without DBD bipolar ionization and a stand-alone HEPA filter

compares the average PM_{10} removal efficiency of the MERV 13 filter assisted with and without DBD bipolar ionization and the HEPA filter alone. The removal efficiency of PM_{10} is calculated similarly using Eq. (1). The MERV 13 filter assisted with DBD bipolar ionization technology improves the PM_{10} removal efficiency (99%) compared with the MERV 13 filter alone without ionization (95%). In addition, Fig. 4 shows concentrations of submicron and micron particle diameters at the controlled case and several air cleaning test configurations with a MERV 13 filter. A controlled case is when neither a fibrous filter nor a DBD bipolar ionizer is used. The MERV 13 filter with the in-duct DBD bipolar ionizer operated demonstrates a comparable reduction in concentrations of submicron and micron particle diameters to the HEPA filter alone. A significant percent reduction (95%) in the concentration of 0.3-μm particle diameter between MERV 13 filter with DBD bipolar ionizer operating and a controlled case can be seen in Fig. 4. Ions from the DBD ionization induce an agglomeration effect on particulate they encounter. Ions are distributed to space via air-handling equipment with the expectation of agglomerating smaller particles into larger particles. This amalgamation of smaller particles into larger particles increases the effectiveness of the filters present in the heating, ventilating, and air conditioning (HVAC) system (larger particles are more easily captured by filters) as well as results in large particles falling out of the air they were previously suspended in. This agglomeration phenomenon increases the effectiveness of the physical air filters installed in the air-handling unit. The larger the particle is, the more easily it is captured by the filter and thus, not returned out into space. Figure 5 presents that the DBD bipolar ionization augments both the particulate matter 2.5 and 10 μm (μm) removal efficiency to be in the upper 80% when an in-duct MERV 8 filter was used. Similarly, Fig. 5 shows a general reduction in particulate concentration when DBD bipolar ionization is activated with a MERV 8 filter compared with a MERV 8 filter with ionization off or in a controlled experiment without using any MERV filter or bipolar ionization.

3.2 Total Volatile Organic Compounds Study. Volatile organic compounds are some of the most common air pollutants emitted from a variety of outdoor sources such as transportation and industrial processes, as well as from indoor sources such as household decorative materials, office printers, etc. [9]. The present study employs a TVOCs sensor (BELIMO) to measure the concentration of TVOCs in terms of percentage. The TVOCs percentage is defined as the ratio of the actual concentration of TVOCs and the maximum possible concentration of TVOCs. One hundred percent is equivalent to 1000 parts per billion (ppb) of TVOCs. DBD bipolar ionization is a nonthermal plasma technology that generates ions, which in turn decomposes toxic VOCs. Figure 6 shows trended TVOCs percentage data with DBD ionization test configuration. The result shows that the DBD bipolar ionization produces an average TVOCs percent reduction of about 40%. A fibrous filter has no effect on the mitigation of VOC concentrations, so their impact on the study is not included.

3.3 Formaldehyde and Carbon Dioxide Study. Both formaldehyde and carbon dioxide gas concentrations do not exhibit significant reductions due to the DBD ionization. Figure 7 shows a minor reduction in the trended concentration data of HCHO gas from the present study with DBD bipolar ionization in operation. The HCHO gas concentration peaks at the end of the source (smoke) injection to the studied indoor air space. However, the reduction in the concentration of HCHO gas is less significant compared with the peaked HCHO gas concentration. Similar findings are found in the work of Park et al. [11] in which the DBD ionization does not have much effect on the removal of HCHO. Figure 8 shows a trended profile of carbon dioxide concentrations with DBD bipolar ionization operating. Owing to oxygen having higher ionization energy than carbon, an insignificant decay of carbon dioxide concentrations was observed in the present study. Thus, DBD ionization does not mitigate carbon dioxide concentration.

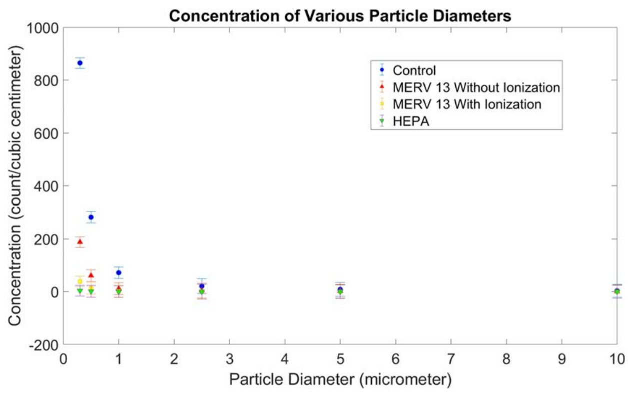

Fig. 4 Concentrations of submicron and micron particle diameters at the controlled case and several air cleaning test configurations with a MERV 13 filter

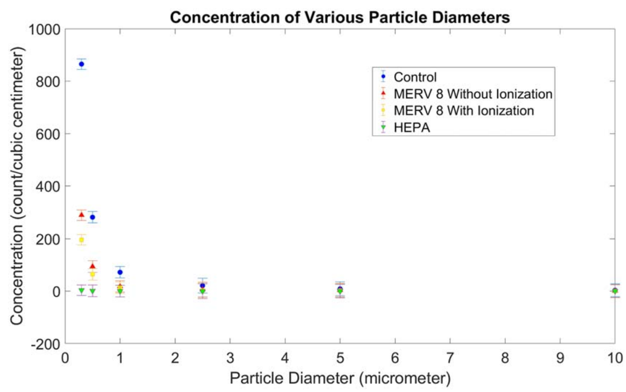

Fig. 5 Concentrations of submicron and micron particle diameters at the controlled case and several air cleaning test configurations with a MERV 8 filter

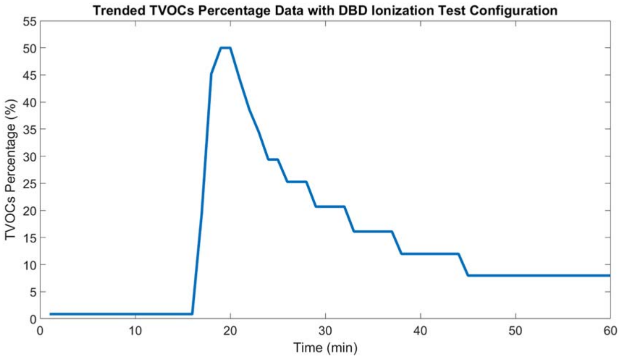

Fig. 6 Trended TVOCs percentage data with DBD ionization test configuration

3.4 Effect of Air Velocity. Figure 9 presents the effect of air velocity on ion concentration with a MERV 13 filter including DBD bipolar ionization. Three air velocities of 3.3 m/s, 6.6 m/s, and 9.5 m/s are reported. The findings show that higher air velocity leads to a greater ion count, which also indicates better air quality as evidenced by the results demonstrated in Fig. 10. At 0.3-μm particle diameter, the percent reduction of particle concentration from the lowest to the highest air velocity is found to be 73%.

3.5 Energy Evaluation Study. The power consumptions of the combined DBD ionization and MERV 13 filtration system and stand-alone HEPA filtration are evaluated and compared. Power consumption is determined using the following equation:

$$\text{Power} = \frac{Q \times \Delta P}{\eta} \tag{2}$$

where Q, ΔP, and η refer to the volumetric airflow rate, airflow resistance in terms of pressure drop across a filter, and combined motor and blower efficiency, respectively. Equation (2) will add the DBD bipolar ionization power in the case of ionization. In the present study, the supply air velocity is measured at 6.6 m/s and the supply air duct diameter is 36 cm. The measured flow resistances of MERV 13 and HEPA filters are 224 Pa and 398 Pa, respectively. The combined motor and blower efficiency is rated at 65%. In addition, the power consumption of the in-duct DBD bipolar ionization device (AtmosAir Solutions FC-400) is 7.68 W. Thus, the power consumptions of the combined DBD ionization and MERV 13 filtration system and stand-alone HEPA filtration are 238.68 W and 411 W, respectively. This finding shows that the HEPA filter uses 42% more power than the combined DBD ionization and MERV 13 filtration system.

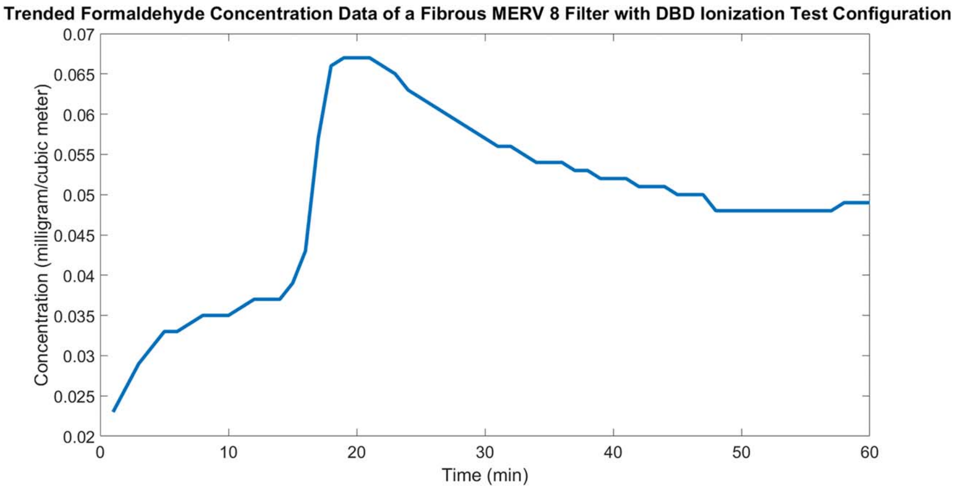

Fig. 7 Trended formaldehyde concentration data with DBD ionization test configuration

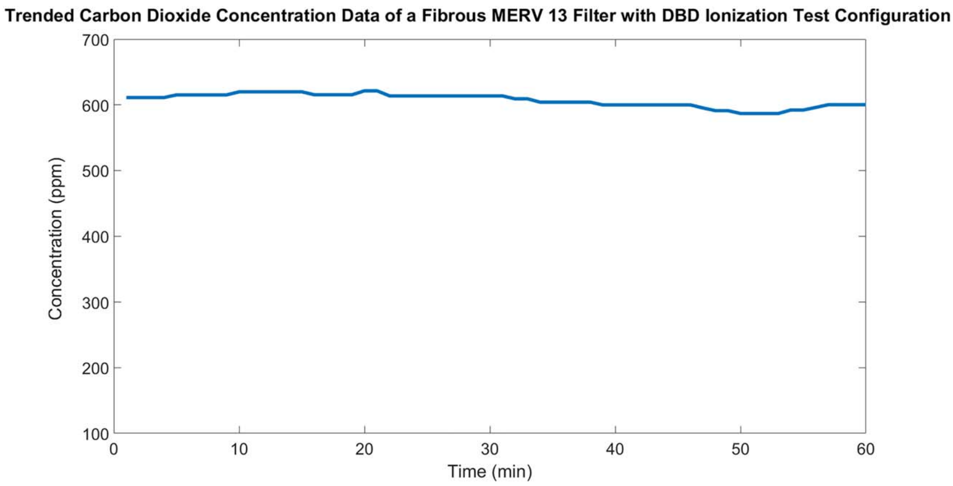

Fig. 8 Trended carbon dioxide concentration data with DBD ionization test configuration

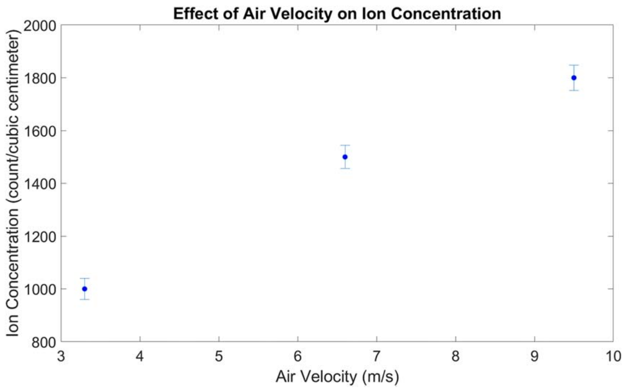

Fig. 9 Effect of air velocity on ion concentration

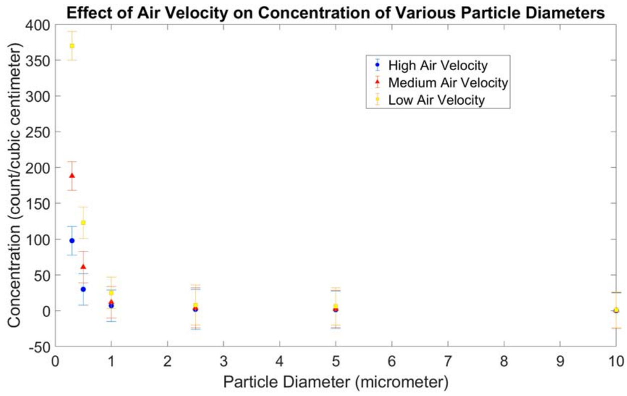

Fig. 10 Effect of air velocity on the concentration of submicron and micron particle diameters with a MERV 13 filter without ionization

4 Conclusions

In summary, the present work studied the effect of a nonthermal plasma technology, DBD bipolar ionization, on the possibility of augmenting a MERV filter to mitigate airborne contaminants that comprise of particulate matter and gaseous pollutants. Experimental results demonstrated that a low-cost MERV filter (e.g., MERV 13) when combined with the DBD bipolar ionizer can approximately attain the particulate removal efficiency of a HEPA filter alone (99.7%). HEPA filter is not optimal as a room air filter because of its high particulate removal efficiency, which is associated with higher electrical power cost and noise (Rudnick 2004). The present work shows that energy consumption due to high pressure drop across a HEPA filter can be conserved, and electrical power costs can be reduced for sustainability. The particulate removal efficiency of $PM_{2.5}$ was 97% when the MERV 13 filter was combined with the DBD bipolar ionization air cleaning device. A significant percent reduction of particulate concentration (95%) at 0.3-μm particle size was reported. In addition, a modest percentage reduction of total volatile organic compounds due to the DBD bipolar ionization also was reported. However, the present study observed only a minor reduction in the concentration of formaldehyde gas with an insignificant reduction in the concentration of carbon dioxide with DBD bipolar ionization operating.

Acknowledgment

The authors acknowledge the ASHRAE San Joaquin for donating the air-handling equipment. Additionally, the authors acknowledge the Lyles College of Engineering at California State University, Fresno, and Fresno City College for providing resources, facilities, and technical support to the present research.

Conflict of Interest

There are no conflicts of interest.

Data Availability Statement

The datasets generated and supporting the findings of this article are obtainable from the corresponding author upon reasonable request.

References

[1] United States Environmental Protection Agency, 2024, "Particulate Matter (PM) Basics," June 20, https://www.epa.gov/pm-pollution/particulate-matter-pm-basics#PM

[2] United States Environmental Protection Agency, 2024, "What Are Volatile Organic Compounds (VOCs)?" March 5, https://www.epa.gov/indoor-air-quality-iaq/what-are-volatile-organic-compounds-vocs

[3] David, E., and Niculescu, V. C., 2021, "Volatile Organic Compounds (VOCs) as Environmental Pollutants: Occurrence and Mitigation Using Nanomaterials," Int. J. Environ. Res. Public Health, **18**(24), p. 13147.

[4] Legg, R., 2017, "Air Filters," Air Cond. Syst. Des., pp. 213–223.

[5] Philips Company, 2018, "Indoor Air Purification and Disinfection," https://www.lighting.philips.com/application-areas/specialist-applications/special-lighting/purification-through-photocatalytic-oxidation, Accessed February 22, 2025.

[6] Byeon, J. H., Hwang, J., Park, J. H., Yoon, K. Y., Ko, B. J., Kang, S. H., and Ji, J. H., 2006, "Collection of Submicron Particles by an Electrostatic Precipitator Using a Dielectric Barrier Discharge," Aerosol Sci., **37**(11), pp. 1618–1628.

[7] BYJU's, 2025, "Electrostatic Precipitator," https://byjus.com/physics/electrostatic-precipitator/, Accessed February 22, 2025.

[8] Breathe Naturally, 2023, "Activated Carbon Filters: What Do They Remove From Your Air?" https://www.breathenaturally.com/blogs/faq/activated-carbon-filters, Accessed February 22, 2025.

[9] Xiao, G., Xu, W., Wu, R., Ni, M., Du, C., Gao, X., Luo, Z., and Cen, K., 2014, "Non-thermal Plasmas for VOCs Abatement," Plasma Chem. Plasma Process., **34**(5), pp. 1033–1065.

[10] Abdel-Salam, M., Hashem, A., Yehia, A., Mizuno, A., Turky, A., and Gabr, A., 2003, "Characteristics of Corona and Silent Discharges as Influenced by Geometry of the Discharge Reactor," J. Phys. D: Appl. Phys., **36**(3), p. 252.

[11] Park, J. H., Byeon, J. H., Yoon, K. Y., and Hwang, J., 2008, "Lab-Scale Test of a Ventilation System Including a Dielectric Barrier Discharger and UV-Photocatalyst Filters for Simultaneous Removal of Gaseous and Particulate Contaminants," Indoor Air, **18**(1), pp. 44–50.

[12] Hobbs, P. C. D., Gross, V. P., and Murray, K. D., 1990, "Suppression of Particle Generation in a Modified Clean Room Corona Air Ionizer," J. Aerosol Sci., **21**(3), pp. 463–465.

[13] Gabbay, J., Bergerson, O., Levi, N., Brenner, S., and Eli, I., 1989, "Effect of Ionization on Microbial Air Pollution in the Dental Clinic," Environ. Res., **52**(1), pp. 99–106.

[14] Lee, B. U., Yermakov, M., and Grinshpun, S. A., 2004, "Removal of Fine and Ultrafine Particles From Indoor Air Environments by the Unipolar Ion Emission," Atmos. Environ., **38**(29), pp. 4815–4823.

[15] Sherali, N. S., 2017, "The Decay of Aerosol Concentration as a Function of Time Comparing the Effects of AHPCO and Bi-polar and an Analysis of Aeroallergens, Fungal Spores and Pollen in the Texas Panhandle Area," Master's thesis, West Texas A&M University, Canyon, TX.

[16] Hyun, J., Lee, S. G., and Hwang, J., 2017, "Application of Corona Discharge-Generated Air Ions for Filtration of Aerosolized Virus and Inactivation of Filtered Virus," J. Aerosol Sci., **107**, pp. 31–40.

[17] Gast, R. K., Mitchell, B. W., and Holt, P. S., 1999, "Application of Negative Air Ionization for Reducing Experimental Airborne Transmission of *Salmonella enteritidis* to Chicks," Poult. Sci., **78**(1), pp. 57–61.

[18] Zeng, Y., Manwatkar, P., Laguerre, A., Beke, M., Kang, I., Ali, A. S., Farmer, D. K., Gall, E. T., Heidarinejad, M., and Stephens, B., 2021, "Evaluating a Commercially Available In-Duct Bipolar Ionization Device for Pollutant Removal and Potential Byproduct Formation," Build. Environ., **195**, p. 107750.

[19] Kim, K.-H., Szulejko, J. E., Kumar, P., Kwon, E. E., Adelodun, A. A., and Reddy, P. A. K., 2017, "Air Ionization as a Control Technology for Off-Gas Emissions of Volatile Organic Compounds," Environ. Pollut., **225**, pp. 729–743.

[20] Van Durme, J., Dewulf, J., Sysmans, W., Leys, C., and Van Langenhove, H., 2007, "Efficient Toluene Abatement in Indoor Air by a Plasma Catalytic Hybrid System," Appl. Catal. B, **74**(1–2), pp. 161–169.

[21] Wu, C. C., and Lee, G. W. M., 2004, "Oxidation of Volatile Organic Compounds by Negative Air Ions," Atmos. Environ., **38**(37), pp. 6287–6295.

[22] Chen, G., Zhang, F., Shen, L., Yi, J., Jiang, P., Wei, Y., Hou, J., et al., 2024, "Formaldehyde Degradation by Soft-Sliding-Electrification-Induced Air Ionization," Nano Energy, **123**, p. 109431.

[23] Rudnick, S. N., 2004, "Optimizing the Design of Room Air Filters for the Removal of Submicrometer Particles," Aerosol Sci. Technol., **38**(9), pp. 861–869.

[24] United States Environmental Protection Agency, 2024, "Setting and Reviewing Standards to Control Ozone Pollution," March 28, https://www.epa.gov/

ground-level-ozone-pollution/setting-and-reviewing-standards-control-ozone-pollution#standards
[25] Kang, K. A., Piao, M. J., Eom, S., Yoon, S.-Y., Ryu, S., Kim, S. B., Yi, J. M., and Hyun, J. W., 2020, "Non-thermal Dielectric-Barrier Discharge Plasma Induces Reactive Oxygen Species by Epigenetically Modifying the Expression of NADPH Oxidase Family Genes in Keratinocytes," Redox Biol., **37**, p. 101698.
[26] United States Environmental Protection Agency, 2024, "What Is a HEPA Filter?" March 5, https://www.epa.gov/indoor-air-quality-iaq/what-hepa-filter#:∼:text=It%20is%20an%20acronym%20for,of%200.3%20microns%20(%C2%B5m)

Hindawi
Indoor Air
Volume 2023, Article ID 6359137, 7 pages
https://doi.org/10.1155/2023/6359137

Research Article

Effects of Ionization on the Filtration of Fine and Ultrafine Particles in Indoor Air

Pranav Muthukrishnan[1] **and Faramarz Farahi**[2]

[1]*Georgia Institute of Technology, North Avenue NW, Atlanta, Georgia 30332, USA*
[2]*Department of Physics and Optical Science, University of North Carolina Charlotte, 9201 University City Blvd., Charlotte, NC 28223, USA*

Correspondence should be addressed to Pranav Muthukrishnan; cmpranav@gmail.com

Received 4 February 2023; Revised 25 May 2023; Accepted 15 June 2023; Published 29 July 2023

Academic Editor: Geun Young Yun

As we spend approximately 80% of our time indoors, improving indoor air quality is necessary to lessen the spread and impacts of respiratory diseases and other health issues caused by particle pollution. Currently, in many countries, the primary method of cleaning indoor air is by using better, higher-grade filters in a recirculating air system or increasing ventilation with outdoor air. One way to supplement these time-tested approaches is by implementing ionization. We used a bipolar ionizer to test the removal efficiency of filters on different particle sizes with and without ionization. Calibrated cigarettes were used to generate smoke into a 28-cubic-meter chamber with a recirculating air handling system. It was found that ionization had a 275% increase in the removal efficiency of the most penetrating particle sizes (100-500 nm). We conclude that ionization drastically improves the filter removal efficiency of fine and ultrafine particles in indoor environments.

1. Introduction

Indoor air quality has been a topic of public and scientific discussion for many years. In a comprehensive study published in 2012 by Lim et al., it was estimated that 3.2 million deaths per year are attributed to ambient particle pollution [1]. The World Health Organization confirmed this estimate while increasing the number to approximately 4 million [2]. Additionally, Horton et al. have shown that climate change will substantially increase the frequency and duration of periods of air stagnation in much of the world, thus leading to higher concentrations of particle pollution as well as other air pollutants [3]. Therefore, improving indoor air quality is becoming increasingly pertinent due to the high level of health issues and mortality rates associated with airborne particle pollution.

Among such particle pollution, fine particulate matter ($PM_{2.5}$) has been identified to cause respiratory diseases [4]. Currently, the most effective method to reduce particulate matter indoors is by using air filters together with increased ventilation. Air filters can be implemented in different ways, including in-room air purifiers with filters or heating, ventilation, and air conditioning (HVAC) systems. There is a wide variation in filter efficiency among the air filters used in HVAC systems. Typically, highly efficient filters such as MERV 16 and HEPA filters are associated with a higher pressure drop that increases over time due to additional loading [5] compared to a lower-rated filter such as MERV 6.

All conventional mechanical air filters are made of microfibers that show good efficiency for large particle sizes but with depleted removal efficiency for particles below 500 nm. In particular, around 300 nm is known as the most penetration particle size (MPPS) for most filters. However, this value typically ranges between 100 and 500 nm, depending on the airflow speed at the filter as well as the diameter and fractional volume of the fibers in the filter. These particles within the ultrafine and submicron ranges are the most harmful to humans due to the risk associated with particle deposition in the respiratory system. For example, the typical size range of allergens is between 0.1 and 0.3 μm; for viruses, it ranges between 0.05 and 0.5 μm; and for wildfire smoke, it is 0.4 to 0.7 μm [6, 7]. As shown in Figure 1 from Kowalski and Bahnfleth, these particle diameter ranges have the lowest filter efficiencies for each of the efficiency curves [8].

In order to improve indoor air quality, it is important to focus on increasing the capture efficiency of these specific particle sizes. Podgorski et al. had found a way to do this by developing and using filters that were composed of nanofibrous as well as microfibrous media [9]. The results of their experiments found that significant increases in filtration efficiency for the MPPS range can be achieved with a moderate rise in pressure drop when utilizing these filters. This method focused on improving the single-fiber deposition efficiency of two of the three mechanisms of deposition (Brownian diffusion and direct interception). The three mechanisms of deposition are impaction, interception, and diffusion; however in addition to improving these three, electrostatic force can also be implemented to improve a filter's performance. This method uses electrostatic interaction between filtration media and particles, therefore, in principle, improving filter performance with no direct effect to the pressure drop. This interaction can be achieved by introducing ions into the air to interact with the particles. The concept of preconditioning particles to increase coagulation has also been used by many others using air ionization [10–17]. All have either used a negative ion generator or a bipolar ion generator.

The focus of this paper is to verify the effect of ionization in improving particle removal efficiency, particularly in the MPPS size range. The data reported is from a series of tests using a bipolar ionizer that is composed of carbon fiber brushes, similar to the systems used by Park et al. as well as Farahi. [14, 15, 18]. The data presented compares the particle removal efficiency of a MERV 10 air filter in an air recirculating HVAC system to that of the same filter when a bipolar ionizer is used to supply both positive and negative ions into the space. The focus of this study is on fine and ultrafine particles [19] produced by a calibrated test cigarette developed by and procured from the University of Kentucky (Kentucky Reference Cigarette # 1 R6F [20]).

2. Experimental Methods

The data presented in this paper was obtained through carefully conducted experiments to examine the effect of needlepoint bipolar ionization on filtration efficiency in a recirculating HVAC system. The current understanding is that when bipolar ionized particles are present in the air, the electrostatic force causes particles of opposite electric charges to attract each other and repel like-charge particles. This attraction-repulsion dynamic is expected to agglomerate ultrafine and fine particles, forming larger particles and thus making it easier for the filter to capture them. This helps to improve the particle removal efficiency of air filters because they typically have very low removal efficiencies for ultrafine and fine particles. The details and conduction of the experiments are described below.

All experiments that are discussed have been conducted in a 28-cubic-meter AHAM room at Blue Heaven Technologies. The air filters used in the trials were 60 cm × 60 cm × 4.5 cm,

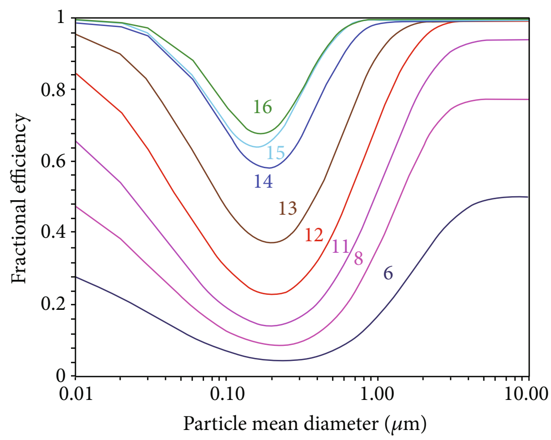

Figure 1: Typical efficiency curve diagram for various rated MERV filters [8].

MERV 10 filters with electret material made by the Aeolus Filter Corporation [21]. The speed of the HVAC recirculating fan was adjusted to achieve 6 air exchanges in the chamber per hour (6 ACH). Following the AHAM standard, a 3-bladed ceiling fan of 36 inches (0.91 m) in length operating at 395 RPM was used to ensure good particle and ion distribution throughout the chamber. A schematic illustrating the experimental setup is shown in Figure 2.

A bipolar ionizer (GPS-FC48™-AC ionization system) that utilizes carbon fiber brushes as ion emitters is mounted in the air supply duct very close to the exit point. The ionizer can be turned on and off remotely as needed. This ionizer has two unipolar electrodes consisting of 48,000 carbon microfibers each, one producing positive ions and the other producing negative ions, with a distance of 2.25 inches (5.625 cm) between them. In order to measure the ion density introduced in the room, an ion counter (Air Ion Counter, AlphaLab, Inc., USA) was mounted on a tripod facing upwards in the middle of the room, 1.5 m from the floor. The ion density was measured in ions/cc of air.

The particle source used was research-grade, calibrated cigarettes from the University of Kentucky that produced a very specific range of particulate sizes from 0.01 to 1.0 μm (PM_1). Researchers have developed methods to introduce a constant level of cigarette smoke into an indoor space [22–25]. As such, the test particles were introduced into the room via the injection port, as shown in Figure 2. This was achieved by attaching a compressed air line to a T-junction. The cigarette was mounted on the second port, and the final port was connected to the tube that feeds into the chamber. Once the cigarette was lit, the compressed air valve is opened, creating a vacuum in the T-junction generated by the forward velocity of the compressed air as it flows through the junction, thus injecting smoke into the chamber. This process ensures an introduction of consistent particle mass and size distribution which is then evenly distributed throughout the chamber using a ceiling fan as previously described.

A TSI DustTrak II Aerosol Monitor and a scanning mobility particle sizer (SMPS) were used to measure the mass and concentration of particles in the chamber. The TSI DustTrak II Aerosol Monitor was placed on the floor

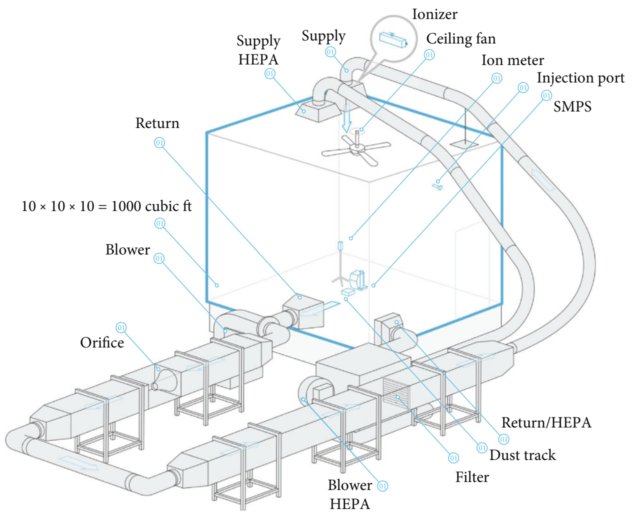

Figure 2: Schematic diagram of the experimental setup in which all controls and tests were conducted.

in the middle of the chamber and was used to measure aerosol concentrations corresponding to PM_1, $PM_{2.5}$, PM_{10}, and mass concentrations ranging from 0.001 to 400 mg per cubic meter with a resolution of ±0.1% for particles in the size range of 0.1 to 10 μm. The SMPS (Model 3938 General SMPS, TSI) was used to capture a detailed particle size distribution from 1 nm to 1000 nm with up to 192 channels. The setup for the SMPS included a cyclone sampler linked by conductive tubing to the SMPS, allowing for aerosolized particles in the room to be captured at the cyclone which was located 1 meter above the floor and delivered to the spectrometer. The SMPS measures the concentration of particles with units of particles per cubic centimeter (#/cc) for particle sizes ranging from 1 nm to 1000 nm recorded as a function of time.

In conducting the experiments, a new filter was first tested with the ionizer turned off. A calibrated cigarette was then used to produce airborne particles, as previously described. Data, including particle counts for various bin sizes and particle mass, was collected over the course of 16 hours. This run will be referred to as the "control" run. Following the control test, the chamber walls were wiped, and a second, separate air recirculating system with a HEPA filter was used to clean the air in the room, as recommended by AHAM. Once the room was cleaned, the recirculating system with the MERV 10 filter was reactivated, the ionizer was turned ON, and the smoke particles were introduced once again. The same data was taken over 16 hours. This run will be referred to as the "treatment" run. These steps were repeated three times with a new filter each time.

In general, such experiments would need to be conducted in a bi-directional crossover fashion, as we know that pre-loading of the filter media will affect the performance of the system. However, this is only impactful if the loading for each trial is high. To confirm this, multiple experiments were executed, sometimes in the reverse order, where we started with the treatment runs first, followed by the control runs. We observed no measurable effect on the results because the particle loading was so low. This is due to the fact that loading from one cigarette had no measurable impact on the filter's performance.

The data used in this paper are from three control and treatment trials in which all conditions were the same except for a new air filter used for each set of control and treatment runs. For the purpose of analysis, the control data used was the average of the three control tests.

3. Theory

In order to properly compare the removal efficiencies for different particle sizes, there must first be a way to model efficiency curves based on properties of the filter such as fiber diameter, thickness, particle speed, and fractional volume of the fiber. There are three main mechanisms that determine filtration efficiencies: diffusion, interception, and impaction [26]. Diffusion is the removal process that dominates when the particle diameter is less than about 0.1 μm [26]. In this particle diameter region, Brownian motion occurs causing the particles to randomly traverse large areas respective to their size which allows for them to attach to a filter fiber. Interception occurs predominantly for particle sizes above 0.1 μm. In this process, a particle is following a normal airflow streamline until it is captured by a fiber in the filter through natural forces [26]. Impaction occurs in much larger particle sizes when a particle's inertia is high enough that it cannot adjust to the changes in the airflow streamline, and so it impacts the filter and is captured [26]. Impaction, however, does not make a significant impact on filter removal efficiency for normal filter velocities [26], and thus it will not be included in the modeling of efficiency curves in this study. Gougeon et al. performed a complex analysis on which equations best modeled the particle penetration in diffusion and interception ranges [27]. They found that Payet's model, Equation (1), best models the penetration in the diffusion regime, while Liu and Rubow's model, Equation (2), best models the penetration in the area where interception is dominant.

$$\eta_D = 1.6125\left(\frac{1-\alpha}{\text{Ku}}\right)^{1/3} Pe^{-2/3} C_d C_d', \quad (1)$$

$$\eta_R = 0.615\frac{1-\alpha}{\text{Ku}}\frac{N_R^2}{1+N_R}C_r, \quad (2)$$

where α is the filter fiber volume fraction (m^3/m^3), Ku is the Kuwabura hydrodynamic factor, Pe is the Peclet number, dimensionless, and N_R is the interception parameter, dimensionless. C_d and C_d' are the diffusion correction factors defined as

$$C_d = 1 + 0.388Kn_f\left(\frac{(1-\alpha)Pe}{\text{Ku}}\right)^{1/3}, \quad (3)$$
$$C'_d = \frac{1}{1+1.6125(1-\alpha/\text{Ku})^{1/3}Pe^{-2/3}C_d},$$

where Kn_f is the Knudsen number (dimensionless) defined as

$$\mathrm{Kn}_f = \frac{2\lambda}{d_f}, \quad (4)$$

where λ is the gas molecule mean free path, 0.067 μm [26]. d_f is the fiber diameter (μm).

C_r is an interception correction factor defined as

$$C_r = 1 + \frac{1.996\mathrm{Kn}_f}{N_R}. \quad (5)$$

The remaining parameters are defined as the following:

$$Ku = a - \frac{a^2 + 2\ln(a) + 3}{4}. \quad (6)$$

a is the total filter media volume (m^3/m^3).

$$\mathrm{Pe} = \frac{1 \times 10^{-6} U d_f}{D_d}, \quad (7)$$

where U is the media face velocity (m/s). D_d is the particle diffusion coefficient (m^2/s).

$$N_R = \frac{D_p}{d_f}, \quad (8)$$

where D_p is the particle diameter (μm).

Once the diffusion and interception efficiencies are calculated, they must be used to calculate single-fiber deposition efficiency by the following equation:

$$\eta = 1 - (1 - \eta_D)(1 - \eta_R). \quad (9)$$

However, the $\eta_D \eta_R$ term is negligible compared to the $\eta_D + \eta_R$ term, and thus can be ignored. Hence, the single-fiber deposition efficiency now becomes

$$\eta = \eta_D + \eta_R. \quad (10)$$

Finally, the overall filter efficiency (E) based on particle size is defined as

$$E = L_u\left(1 - e^{-\eta S}\right), \quad (11)$$

where L_u is a multiplicative correction factor [8] and S is the fiber projected area, dimensionless, defined as

$$S = \frac{4L\alpha}{\pi d_f (1 - \alpha)} \quad (12)$$

where L is the length of filter media in direction of airflow (μm).

Additionally, Podgorski et al. had stated that pressure drop, Δp, can be estimated as

$$\frac{\Delta p}{L} = \frac{64\mu U}{d_f^2}\alpha^{3/2}\left(1 + 56\alpha^3\right). \quad (13)$$

The pressure drop created by the filter is due to its resistive force. The higher the pressure drop, the higher the force, and as a result, more energy is required to push the particles through the filter. As is well known, this force causes a change in the momentum of the particles. This is why a particle's speed is lower inside the media than the speed of the same particle before reaching the filter. In the treatment runs, there is an additional electrostatic force that is acting on the charged particles that also impacts the speed of particles in the filter media. This further reduces the particles' speed without causing any pressure drop. This allows for smaller size particles to be captured by the filter through diffusion and electrostatic force.

The equations above are for single-fiber filters; however, the majority of filters utilize multifibrous media, and thus there needs to be a way to model these kinds of filters. Kowalski et al. have developed such a method in which Equations (1) and (2) are calculated for each fiber [26]. Thus, any reference to fiber diameter, d_f, or fiber fractional volume, α, has now become specific to each individual fiber and must be calculated for every fiber in the filter. For instance, Equation (12) for the fiber project area would now become

$$S_i = \frac{4L\alpha_i}{\pi d_{f,i}(1 - \alpha_i)}. \quad (14)$$

Once the single-fiber efficiencies, η_i, and fiber projected area, S_i, are calculated for each of the fibers, the overall filter efficiency (Equation (11)),

$$E = 1 - e^{-\sum \eta_i S_i}. \quad (15)$$

It is now possible to vary the values for the fiber diameters and the fiber volume fractions for the filter efficiency curve to match the data from the experiments that were previously outlined. However, there are some restrictions used when varying these values. Most highly rated filters consist of fiber diameters between 0.65 and 6.5 μm, Kowalski et al. [26], so we restricted the fiber diameter values to be within this range. Additionally, the fiber volume fractions must all add to 1. For the purpose of this study, the assumption was made that there are three fibers with different fiber diameters. Table 1 summarizes the parameters used in modeling the efficiency curves.

However, fitting such a curve to the treatment data shows that there is not a strong correlation between the expected curve and the data. As shown in Figure 3, the treatment data with error bars does not look like a typical filter efficiency curve, and we can see that ionization effects diffusion and interception removal processes differently. So instead, for the purpose of getting agreement between theory and experiments, we chose to look at diffusion and interception efficiencies separately, varying the values for fiber

Table 1: Multifiber filter model parameters for diffusion and interception.

Parameters	Control diffusion	Control interception	Treatment 1 interception	Treatment 2 interception	Treatment 3 interception
Total volume fraction α	0.0020	0.0020	0.0020	0.0020	0.0020
Media length (m)	0.015	0.015	0.015	0.015	0.015
Nominal face velocity (FPM)	25	25	25	25	25
Media velocity (FPM)	3.118914308	3.118914308	3.118914308	3.118914308	3.118914308
Media velocity (m/s)	0.015840093	0.015840093	0.015840093	0.015840093	0.015840093
Fiber 1 diameter (microns)	3.32	2.00	0.771	0.80	0.827
Fiber 1 fraction of total α	0.33	0.94	0.44	0.60	0.57
Fiber 2 diameter (microns)	4.78	6.00	2.01	2.22	2.40
Fiber 2 fraction of total α	0.29	0.03	0.35	0.23	0.30
Fiber 3 diameter (microns)	6.45	6.50	5.75	5.60	6.50
Fiber 3 fraction of total α	0.38	0.03	0.21	0.17	0.13
Multiplication coefficient, L_u	1.00	0.95	0.965	0.93	0.946
r^2	0.89	0.82	0.98	0.98	0.96

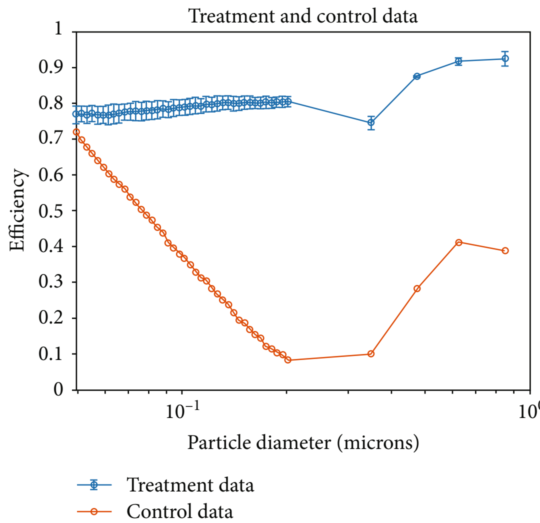

Figure 3: Removal efficiency of control versus treatment data.

diameters and fiber volume fractions to get as high of a correlation coefficient as possible between the curve and the data points. For the diffusion region, the correlation coefficient was determined from the data points between 49.6 nm and 350 nm, while for the interception efficiency, the value was determined from the data points between 350 nm and 850 nm. While the efficiency curve formula that was previously described could accurately model the diffusion region of the control data, the treatment data within the same region no longer behaved this way. Instead, it was found that a quadratic fit best modeled this portion of the treatment data. The parameters we found that best match our data are shown in Table 1. Once the diffusion and interception curves were optimized to best fit the data, the intersection between the curves was found, and a rolling average was taken from 10 nm from each side of the intersection point to smooth the curve.

With this new curve, we can accurately find the average efficiency by taking the area under the curve for a specific region and dividing that value by the difference between the highest and lowest particle diameter values in that region.

4. Results

These such curves are used to determine ratings for filters based on the removal efficiency for three different particle ranges: 0.3 to 1.0 μm, 1.0 to 3.0 μm, and 3.0 to 10.0 μm. For the purposes of the study, we are interested in finding the average efficiency between control and treatment data for these particle size ranges as well as the MPPS range. Once the optimized curves were developed, the curve was integrated to get the area underneath in order to find the average efficiency for a certain particle diameter range. This area was then divided by the difference between the highest and lowest particle diameters in that range. The process was done for each curve for the previously specified particle size ranges. The results of which are displayed in Table 2.

As can be seen from this table, there is a significant increase in filter removal efficiency in the 0.3-1 micron range, including the MPPS range, by implementing ionization. When considering the average efficiencies of the three treatment trials, there is a 275 percent increase in removal efficiency for the MPPS range of 100-500 nm.

5. Discussion

Substantial particle removal efficiency was achieved by implementing an ionizer to produce 20,000 ± 500 positive and negative ions prior to the cigarette smoke being introduced into the chamber. Once the smoke was introduced, the ion count drastically decreased since the ions were polarizing the smoke particles which led to the agglomeration of these particles. There was a 134 percent increase in the removal efficiency of particles in the 0.3-1.0 micron range

Table 2: Combined diffusion and interception average efficiency data.

	Control	Treatment 1	Treatment 2	Treatment 3	Average treatment
Overall r^2	0.87	0.99	0.97	0.98	N/A
0.3-1 micron	0.384	0.899	0.888	0.887	0.892
1-3 micron	0.847	0.965	0.930	0.946	0.947
3-10 micron	0.949	0.965	0.930	0.946	0.947
MPPS value (microns)	0.2956	0.3417	0.3421	0.3403	0.3414
MPPS efficiency	0.221	0.797	0.818	0.790	0.802

when ionization was used and a 275 percent increase in the MPPS range of 100-500 nm (Table 2). It was observed that with the use of ionization, the most penetrating particle size had increased in diameter. Thus proving that when the particles present in the air are ionized with both positive and negative charges, the attraction-repulsion dynamic results in the coagulation of particles with opposite charges, leading to a higher concentration of larger diameter particles. These larger particles are then more easily captured by the filter either through interception or electrostatic attraction. However, even the most efficient filters have a most penetrating particle size, which ionization can help improve the capture efficiency.

Additionally, larger particles are subjected more to gravitational force since they have a higher mass. Thus, if the gravitational force exerted on the particle is greater than the electric force, then the particle is more likely to deposit onto a surface rather than the filter.

As previously stated, every filter creates a pressure drop caused by its resistive force. Typically, more efficient filters are more fibrous and thus have a higher resistive force which creates a greater pressure drop. This force decreases a particle's momentum within the filter which results in a lower velocity of the particle through the filter. This lower velocity allows for smaller particles to be more easily captured through the diffusion process. Through the use of bipolar ionization, there is an additional electrostatic force that is acting on the charged particles. This force opposes the motion of the particles and thus further reduces the speed of the particles within the filter media. Smaller size particles are more easily captured through diffusion and electrostatic force. Therefore, as shown, the use of a bipolar ionizer improves a filter's removal efficiency to that of a higher-rated filter without increasing the resistive force. The resultant pressure drop across the filter remains the same, and the energy required to push particles through the filter is the same.

6. Conclusion

The results of this study confirm that bipolar ionization increases a mechanical filter's removal efficiency of fine and ultrafine particles from indoor environments as well and more information on how ionization affects the most penetrating particle sizes. The ionizer used in this study produced an average 275% increase in the removal efficiency of the MPPS range after 18 minutes when compared to the control. Therefore, the use of bipolar ions to help clean indoor air has proven to be an effective method. This process can then be applied and tested in cleaning efficiencies for other air pollutants such as wildfire smoke. In areas where there are many and spontaneous wildfires, this technology can be especially useful.

Data Availability

Unfortunately, due to a nondisclosure agreement (third-party agreement) between the authors and collaborators, the authors cannot disclose the data.

Conflicts of Interest

The authors declare that they have no conflicts of interest.

Acknowledgments

The authors would like to acknowledge the financial support of GPS Air in conducting this research. Pranav Muthukrishnan would like to thank GPS Air for a Summer Internship.

References

[1] S. S. Lim, T. Vos, A. D. Flaxman, G. Danaei, K. Shibuya, and H. Adair-Rohani, "A comparative risk assessment of burden of disease and injury attributed to 67 risk factors and risk factor clusters in 21 regions, 1990-2010: A systematic analysis for the global burden of disease study 2010," *The Lancet*, vol. 380, no. 9859, pp. 2224–2260, 2013.

[2] World Health Organization, *World Report on Knowledge for Better Health: Strengthening Health Systems*, World Health Organization, 2004.

[3] D. E. Horton, C. B. Skinner, D. Singh, and N. S. Diffenbaugh, "Occurrence and persistence of future atmospheric stagnation events," *Climatic Change*, vol. 4, no. 8, pp. 698–703, 2014.

[4] G. Sérafin, P. Blondeau, and C. Mandin, "Indoor air pollutant health prioritization in office buildings," *Indoor Air*, vol. 31, no. 3, pp. 646–659, 2021.

[5] S. N. Rudnick, "Optimizing the design of room air filters for the removal of submicrometer particles," *Aerosol Science and Technology*, vol. 38, no. 9, pp. 861–869, 2004.

[6] "Why wildfire smoke is a health concern," https://www.epa.gov/wildfire-smoke-course/why-wildfire-smoke-health-concern.

[7] E. Alonso-Blanco, A. I. Calvio, R. Fraile, and A. Castro, "The influence of wildfires on aerosol size distributions in rural

areas," *The Scientific World Journal*, vol. 2012, Article ID 735697, 13 pages, 2012.

[8] W. J. Kowalski and W. Bahnfleth, "Merv filter models," 2002, https://www.nafahq.org/merv-filter-models/.

[9] A. Podgórski, A. Bałazy, and L. Gradoń, "Application of nanofibers to improve the filtration efficiency of the most penetrating aerosol particles in fibrous filters," *Chemical Engineering Science*, vol. 61, no. 20, pp. 6804–6815, 2006.

[10] Z. Grabarczyk, "Effectiveness of indoor air cleaning with corona ionizers," *Journal of Electrostatics*, vol. 51-52, pp. 278–283, 2001.

[11] J. Černecký, K. Valentová, E. Pivarčiová, and P. Božek, "Ionization impact on the air cleaning efficiency in the interior," *Measurement Science Review*, vol. 15, no. 4, pp. 156–166, 2015.

[12] B. Pushpawela, R. Jayaratne, A. Nguy, and L. Morawska, "Efficiency of ionizers in removing airborne particles in indoor environments," *Journal of Electrostatics*, vol. 90, pp. 79–84, 2017.

[13] S. A. Grinshpun, A. Adhikari, B. U. Lee, M. Trunov, and E. A. G. Mainelis, "Indoor air pollution control through ionization," *WIT Transactions on Ecology and the Environment*, vol. 74, 2004.

[14] J.-H. Park, K.-Y. Yoon, Y.-S. Kim, J. H. Byeon, and J. Hwang, "Removal of submicron aerosol particles and bioaerosols using carbon fiber ionizer assisted fibrous medium filter media," *Journal of Mechanical Science and Technology*, vol. 23, no. 7, pp. 1846–1851, 2009.

[15] J. H. Park, K. Y. Yoon, and J. Hwang, "Removal of submicron particles using a carbon fiber ionizer-assisted medium air filter in a heating, ventilation, and air-conditioning (HVAC) system," *Building and Environment*, vol. 46, no. 8, pp. 1699–1708, 2011.

[16] M. Smith, K. Lee, and T. Matsoukas, "Coagulation of charged aerosols," *Journal of Nanoparticle Research*, vol. 1, no. 2, pp. 185–195, 1999.

[17] S. M. Charan, W. Kong, R. C. Flagan, and J. H. Seinfeld, "Effect of particle charge on aerosol dynamics in Teflon environmental chambers," *Aerosol Science and Technology*, vol. 52, no. 8, pp. 854–871, 2018.

[18] F. Farahi, "Soft ionization: improving indoor air quality," *IEEE Transactions on Industry Applications*, pp. 1–7, 2023.

[19] EPA, "Particle pollution exposure," https://www.epa.gov/pmcourse/particle-pollution-exposure.

[20] "Center for tobacco reference products," https://ktrdc.ca.uky.edu/Reference-Products.

[21] "Aeolus corporation," https://aeoluscorp.com/.

[22] N. E. Klepeisn, M. Apte, L. A. Gundel, R. G. Sextro, and W. W. Nazaroff, "Determining size-specific emission factors for environmental tobacco smoke particles," *Aerosol Science and Technology*, vol. 37, no. 10, pp. 780–790, 2003.

[23] D. Mueller, J. Schulze, H. Ackermann, D. Klingelhoefer, S. Uibel, and D. A. Groneberg, "Particulate matter (pm) 2.5 levels in ets emissions of a Marlboro red cigarette in comparison to the 3r4f reference cigarette under open- and closed-door condition," *Journal of Occupational Medicine and Toxicology*, vol. 7, no. 1, p. 14, 2012.

[24] X. Tang, Z. Zheng, H. S. Jung, and A. Asa-Awuku, "The effects of mainstream and sidestream environmental tobacco smoke composition for enhanced condensational droplet growth by water vapor," *Aerosol Science and Technology*, vol. 46, no. 7, pp. 760–766, 2012.

[25] M. Forster, J. McAughey, K. Prasad, E. Mavropoulou, and C. Proctor, "Assessment of tobacco heating product thp1.0. Part 4: characterisation of indoor air quality and odour," *Regulatory Toxicology and Pharmacology*, vol. 93, pp. 34–51, 2018.

[26] W. J. Kowalski, W. P. Bahnfleth, and T. S. Whittam, "Filtration of airborne microorganisms: modeling and prediction," *ASHRAE Transactions*, vol. 105, 1999.

[27] R. Gougeon, D. Bouland, and A. Renoux, "Comparison of data from model fiber filters with diffusion, interception and inertial deposition models," *Chemical Engineering Communications*, vol. 151, no. 1, pp. 19–39, 1996.